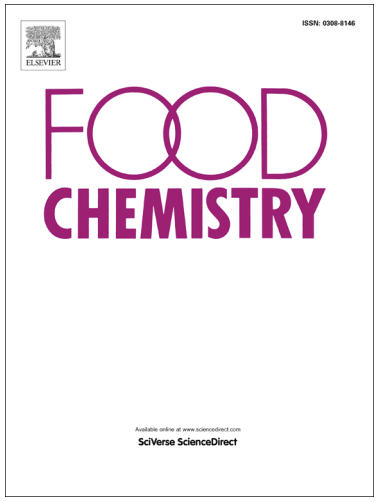

Monitoring chemical changes during food sterilisation using ultrahigh resolution mass spectrometry

James W. Marshall, Philippe Schmitt-Kopplin, Nadine Schuetz, Franco Moritz, Chloé Roullier-Gall, Jenny Uhl, Alison Colyer, Lewis L. Jones, Michael Rychlik, Andrew J. Taylor

PII: S0308-8146(17)31540-6
DOI: http://dx.doi.org/10.1016/j.foodchem.2017.09.074
Reference: FOCH 21743

To appear in: *Food Chemistry*

Received Date: 16 June 2017
Revised Date: 5 September 2017
Accepted Date: 13 September 2017

Please cite this article as: Marshall, J.W., Schmitt-Kopplin, P., Schuetz, N., Moritz, F., Roullier-Gall, C., Uhl, J., Colyer, A., Jones, L.L., Rychlik, M., Taylor, A.J., Monitoring chemical changes during food sterilisation using ultrahigh resolution mass spectrometry, *Food Chemistry* (2017), doi: http://dx.doi.org/10.1016/j.foodchem.2017.09.074

Monitoring chemical changes during food sterilisation using ultrahigh resolution mass spectrometry

James W. Marshall[a]*, Philippe Schmitt-Kopplin[b], Nadine Schuetz[a], Franco Moritz[b], Chloé Roullier-Gall[b], Jenny Uhl[b], Alison Colyer[a], Lewis L. Jones[a], Michael Rychlik[c] and Andrew J. Taylor[a]

[a] WALTHAM Centre for Pet Nutrition, Mars Petcare, Waltham on the Wolds, Leicestershire LE14 4RT, United Kingdom

[b] Helmholtz Zentrum Muenchen, Analytical BioGeoChemistry, Ingolstaedter Landstr. 1, 85764 Neuherberg, Germany

[c] Chair of Analytical Food Chemistry, Technical University of Munich, Alte Akademie 10, 85354 Freising, Germany

*Corresponding author: email james.marshall@effem.com; Fax +44 1664 415440

Abstract

Sterilised food products undergo chemical changes during processing that ultimately determine the product quality. To provide detailed information on the chemistry of each stage of a pet-food sterilisation process, a laboratory-scale system was developed, which allowed sampling under the high temperatures and pressures associated with sterilisation. Products from the laboratory-scale system were representative of the factory process. Sample extracts were analysed by Fourier Transform-Ion Cyclotron Resonance-Mass Spectrometry (FT-ICR-MS), which delivered the molecular formulae and ion intensities of the compounds present. Data were examined to determine the coverage of this method, the degree of chemical change occurring during pet food thermal processing, and the level of identification possible with FT-ICR-MS. Data visualisation and statistical analysis identified significant chemical changes in pet food as a result of processing, and allowed tentative identification of the compounds involved. Insights generated using FT-ICR-MS analysis can be confirmed and further explored using conventional, targeted analyses.

Proposed running title “Monitoring chemical changes during food sterilisation”,

Keywords: Maillard reaction, van Krevelen, data visualisation, data mining FT-ICR-MS

This research did not receive any specific grant from funding agencies in the public, commercial, or not-for-profit sectors.

1. Introduction

A key objective of food manufacturers is to produce consistent product quality against a background of variability in raw materials and variability in processing. Variability in raw materials may be due to seasonal or market-led factors, while variability in processing can result from factors like different manufacturing equipment in different geographical locations. Chemical changes that occur during food processing are ultimately responsible for changes in product quality attributes like nutrition, colour and flavour. The scientific literature shows that thermal processing of food initiates a wide range of sequential and interconnected chemical reactions that have historically proved difficult to unravel (see for example Davidek, Velisek, & Pokorny, 1990).

Most of the quality changes are due to the generation of reactive low molecular weight compounds (<1000 Da) formed from naturally-occurring food components like sugars or amino acids during processing. Researchers have tended to study the reaction pathways individually, but it is well-known that significant interactions take place between products from the different pathways. An example is the production of species-specific meat flavours when the lipid oxidation and the Maillard pathways interact (Mottram, 1998). However, other chemical species like hydroxycinnamic acids can also affect the Maillard reaction (Moskowitz & Peterson, 2010) and, to gain a full picture of the chemical changes occurring in a real food during processing, it is necessary to monitor many classes of compounds. In some well-defined and well-controlled studies, flavour changes driven by the Maillard reaction have been successfully monitored. For example, aroma generation during coffee roasting in small-scale roasters was monitored as a function of the starting chemical composition and as a function of process conditions (Lindinger, Labbe, Pollien, Rytz, Juillerat, Yeretzian, et al., 2008; Yeretzian, Jordan, Badoud, & Lindinger, 2002).

1.1 Processing requirements

The ambition of this study was to monitor as wide a variety of chemical compounds as possible (excluding macromolecules) during the sterilisation of a “wet” pet food. Pet food manufacture starts with the manufacture of meat chunks from animal by-products. Gravy or jelly is then added to the chunks before sterilisation at 120-130 ^{o}C for 30-60 min. Monitoring the chemical changes during the process would provide detailed information on the course and extent of the chemical reactions but, because the food is sealed in a can or a pouch, sampling is usually restricted to before or after processing. One way to avoid the need for direct sampling is to prepare a series of small samples in sealed glass vials and heat them for different times. Each sample is then analysed and a plot of chemical changes against sterilisation time is built from the individual data (see for example Balagiannis, Howard, Parker, Desforges, & Mottram, 2010). For large-scale experiments, this technique is laborious and time-consuming and does not allow sufficient replicates and samples to be studied to understand the variation in processing. An alternative approach is to use commercially available, small-scale pressure reactors to mimic food thermal processing and provide direct sampling during processing (Chu & Doyle, 1999; Guan, Wang, Yu, Yu, & Zhao, 2012; Hwang, Shahidi, Onodenalore, & Ho, 1997; Wang, Yang, & Song, 2012). A system that mimicked the pet food sterilisation, time-temperature profile and also allowed sampling under pressure was developed to allow the chemistry occurring during sterilisation to be studied.

1.2 Chemical analysis requirements

Assuming samples can be taken during sterilisation, the next challenge is to analyse the wide range of chemical classes present in the food, so that changes in the chemical pathways can be observed. Using conventional analytical techniques, each chemical class requires its own equipment and methods, requiring optimization, validation, replication, stability studies *etc*. Compound identification and quantification are also very time-consuming activities and, therefore, there are limits on the number of compounds that can be realistically monitored in complex systems like pet foods using conventional chemical analyses. Data processing is yet another significant task. Each analysis will provide information about changes in that particular class of compounds (e.g. in sugars, fatty acids or amino acids). It is then necessary to combine data from the different analyses in order to identify chemical reaction pathways (or relationships between compounds) from which a fundamental understanding of the chemical pathways that are taking place in the process steps could be elucidated.

Since there are parallels between the analysis of biological processes on a molecular level (metabolomics) and the analysis of chemical changes during processing, analytical methods typically used in the metabolomics area were assessed. A recent review describes the challenges needed to extract a wide range of small molecular weight, relatively polar molecules using a simple extraction procedure and an analytical system with wide compound coverage (Clark, Zhang, & Anderson, 2016). Untargeted Fourier Transform-Ion Cyclotron Resonance-Mass Spectrometry (FT-ICR-MS) was selected for this study as it allows direct infusion of sample extracts into an ion source with no chromatography, thus allowing rapid analysis and high sample throughput. Different ionisation sources can be used to optimize the analysis for the various chemical compounds, moreover, the accurate mass values obtained, allow more confident prediction of the molecular formulae, which provides a good first step towards compound identification.

Some preliminary studies on the application of high resolution mass spectrometry to food products have been published, however, they have tended to target specific chemical classes like the total and oxidised lipids in caviar (Porcari, Fernandes, Belaz, Schwab, Santos, Alberici, et al., 2014), checking whisky for ageing, counterfeiting and adulteration (Garcia, Vaz, Corilo, Ramires, Saraiva, Sanvido, et al., 2013), the adulteration of coffee (Garrett, Vaz, Hovell, Eberlin, & Rezende, 2012), thearubigin formation in tea (Kuhnert, Drynan, Obuchowicz, Clifford, & Witt, 2010) and vegetable oil characterisation (Wu, Rodgers, & Marshall, 2004). A preliminary study on Maillard products measured the reaction of a sugar with different amino acids in a simple model system (Golon, Kropf, Vockenroth, & Kuhnert, 2014). A comparative analysis of two cocoa bean samples was successful in identifying compounds containing CHO, CHNO and CHNO, which were identified as lipids, carbohydrates and peptides (Milev, Patras, Dittmar, Vrancken, & Kuhnert, 2014). A comprehensive study that monitored the chemical profile through the whole winemaking process, was able to identify the origin of some key wine compounds at specific processing steps, and in response to specific environmental factors, like the vineyard location and the vintage (Roullier-Gall, Lucio, Noret, Schmitt-Kopplin, & Gougeon, 2014).

1.3 Aims and objectives

The first purpose of this study was to validate a small-scale process for pet food sterilisation against the standard factory process to ensure that the same quality of product was produced in both

systems. Validation used both conventional chemical and sensory analyses. The second purpose was to assess FT-ICR-MS and the data it provides. The outputs of FT-ICR-MS are accurate mass data, predicted molecular formulae and ion intensity. Molecular formulae do not provide unequivocal compound identification, as many geometric- and stereo-isomers can exist for one molecular formula. Key questions for this study were: what resolution and coverage of the varied chemical classes in pet food could be achieved; could van Krevelen diagrams (Milev, Patras, Dittmar, Vrancken, & Kuhnert, 2014) help visualise chemical relationships between analytes/samples and what level of compound identification could be obtained simply by accurate mass measurement? If FT-ICR-MS analysis and subsequent data processing could identify tentative identifications and chemical relationships, then conventional, targeted techniques could be applied to study these specific parts of the chemical pathways.

2. Materials and Methods

2.1 Materials

All solvents (methanol, hexane, water) were HPLC grade and obtained from SigmaAldrich (Poole, UK).

2.2 Laboratory-scale sterilisation

Sterilisation of pet food took place in a bench top reactor system (4520; Parr Instrument Company, Illinois, USA) coupled to a 4848 controller. The standard Parr steel vessel (1 L) was fitted with an electrical heating jacket, anchor-type stirring blades and a Parr sampling system. Un-sterilised product (meat chunks in gravy; typical proximate analysis moisture 84 g/100 g, protein 8.6 g/100 g, fat 4.8 g/100 g) was obtained from the local Mars Petcare factory (Melton Mowbray, UK). Two samples of the factory-sterilised product (made from the same chunk/gravy batch) were also obtained for comparative analysis. Three separate sterilisation runs were carried out, each with 800 g of un-sterilised product, which was placed in the 1 L Parr steel vessel and briefly homogenised (1 min) to avoid meat chunks blocking the sampling system. A 10-g sample was taken to represent time zero, then the vessel was closed, stirred at 6 rpm using the impeller, heated to 125 °C, held to achieve the desired f_0 value and then cooled to room temperature using ice. Samples (10 mL) were taken before and after processing (t_0 and t_6) and at five time intervals (t_1 to t_5) during the sterilisation process (using the Parr sampling system) and frozen (-18 °C) immediately. In total, 21 samples were produced for analysis, across three replicate sterilisation processes, each with seven time points between t_0 and t_6.

2.3 Validation of laboratory-scale and factory-scale processing

To ensure the fully-processed samples (t_6) from the Parr Reactor were comparable to the factory-produced product, the odour of both samples was assessed using chemical and sensory analyses. The rationale was that odour would be more sensitive to chemical changes caused by differences between the Parr and factory sterilisation systems.

2.3.1 SPME-GC headspace volatile analysis

The headspace of factory and small-scale pet food samples (6 g) was sampled (55 min at 35 °C) using a solid phase micro extraction (SPME) device (Supelco, Bellefonte, PA, USA) fitted with a 50/30 µm (DVB/CAR/PDMS) fibre. Fibres were desorbed into a GC-MS (7890A, 5975C; Agilent Technologies,

Palo Alto, CA) at 200 °C in splitless mode and chromatographed on a ZB-FFAP capillary column (Phenomenex, USA; 30 m, 0.25 mm i.d., film thickness 0.25 µm) with a temperature program (35 °C for 2 min, then 2 °C/min to 125 °C, then 10 °C/min to 240 °C and finally 240 °C for 2 min). Electron impact (70 eV) mass spectra were obtained in the range 30–300 amu. Retention times and mean values (6 replicates of each product) for the percentage peak areas in both the laboratory-scale and factory-scale samples were recorded and comparisons made using Dunnett's multiple comparison method (Dunnett, 1955) at a 5% significance level using Statgraphics (Centurion XVI, Warrenton, VA, USA).

2.3.2 Analysis of aroma-active compounds by GC-Olfactometry

Volatile compounds were extracted in duplicate from the factory and fully processed laboratory product (t_6) using Solvent Assisted Flavour Evaporation (SAFE) (Engel, Bahr, & Schieberle, 1999). Homogenised sample (10 g) was extracted with 100 mL diethyl ether, centrifuged (5000 rpm, 10 °C, 10 min) and re-extracted with 50 mL diethyl ether. The volume was reduced using a Vigreux column and micro-distillation to 250 µL and stored at -80 °C until analysis. Aliquots (1 µL) were injected onto a GC-O-MS system (Agilent 7890A GC fitted with a FFAP column (as above) and an Olfactory Detection Port) and the eluted peaks sniffed by a trained assessor. Retention times of odorous compounds and their odour intensities were recorded (scale; 1- very weak to 10 – very strong).

2.3.3 Sensory analysis

Two separate batches of each of the factory (A) and fully-processed laboratory (B) product were homogenised, and 15 g aliquots weighed into capped glass vials covered with paper to mask any visual differences and labelled with randomised 3 digit codes. Twenty-six trained panellists were presented with their own set of samples in each of the six possible orders (ABB, BAB, BBA, AAB, ABA or BAA) and carried out a forced choice Triangle Test (ISO 4120:2004).

Each panellist was randomly assigned to a presentation order with assessment taking place in individual, red-lit booths in a sensory panel room (ISO_8589;2007 (E)). Each assessor sniffed the three samples and marked the one that was different. Assessors were allowed to retry the three samples following the same presentation order and were given 5-min rest periods between sample groups. FIZZ software analysed the results, comparing the proportion of correct responses to chance (p=1/3), using a one sample binomial test with a α-risk of 5% and using the appropriate statistical tables (Kemp, Hollowood, & Hort, 2009).

2.4 Sample extraction for FT-ICR-MS analysis

Samples (5 g, t_0 to t_6) taken from the Parr reactor were homogenised with methanol:water (1:1; 20 mL) and hexane (10 mL). The hexane phase containing the triglyceride fraction was separated by centrifugation (11,000 *g*). An aliquot (4 mL) of the methanol-water phase was dried (SpeediVac, Thermo Fisher Scientific, Loughborough, UK) then sealed and stored at room temperature. Prior to uHRMS analysis, samples were reconstituted in HPLC grade water (2 mL), centrifuged and then filtered through a SFCA syringe filter (0.2 µm; Thermo Fisher Scientific).

2.5 FT-ICR-MS

High resolution mass spectra were measured on a Fourier Transform Ion Cyclotron Resonance Mass Spectrometer (FT-ICR-MS, SolariX TM, Bruker Daltonics GmbH, Bremen, Germany) equipped with a 12 Tesla superconducting magnet (Magnex Scientific Inc., Yarnton, GB) and an APOLLO II

electrospray ionisation (ESI) source (Bruker Daltonics GmbH, Bremen, Germany). Sample extracts were diluted in pure methanol (1:100) prior to injection and introduced into the micro electrospray source at a flow rate of 120 µL/h. FT-ICR-MS background and calibration were carried out as before (Roullier-Gall, Lucio, Noret, Schmitt-Kopplin, & Gougeon, 2014) and spectra were acquired in negative ionisation mode accumulating 400 scans within the *m/z* range of 90-1000 and with a time domain of 4 megawords.

2.6 Data analysis

Accurate mass calibration of mass spectra was carried out using DataAnalysis 4.0 (Bruker Daltonics) on a list of fatty acids and other persistent, recurrent compounds universally present in the FT-ICR-MS spectra of the samples. Calibration was linear up to *m/z* 600, with mass error below 0.05 ppm. Acquired masses were filtered to remove signals < 6 times signal-to-noise ratio and a relative intensity threshold of less than 0.001%. To carry out statistical analysis, the raw data peaks were aligned across all samples using in-house software (Matrix Generator; maximum error 1.0 ppm). The data matrix was processed to assign formulae (Roullier-Gall, Lucio, Noret, Schmitt-Kopplin, & Gougeon, 2014), annotate known metabolites and remove spectra which could not be explained by combinations of CHNOPS given z = 1.

2.7 Statistical analysis and visualisation

Statistical evaluation of changes in ion intensity for a specific molecular formula between time points in the sterilisation process was carried out using linear mixed models. These were performed on the log10 (+1) raw data, for each formula, with replicate as a random effect and time as a fixed categorical effect. Where this model did not converge, the random effect of replicate was dropped from the model. All pairwise time points were compared and *p*-values were adjusted using a false discovery rate correction (Benjamani-Hochberg) to 5% within each comparison. H:C, O:C and N:C ratios were calculated from the molecular formulae and data plotted as van Krevelen diagrams using Spotfire® (Tibco, Palo Alto, Ca, USA) to visualise the relationship between molecular formulae, elemental composition and ion intensities.

3. Results

3.1 Validation of the Laboratory sterilisation method

Pet food samples from the factory and from the small-scale system (made with the same ingredients) were compared using chemical and sensory tests. Volatile compounds were targeted as they were hypothesised to be more sensitive to chemical change than the general non-volatile compounds and they are also responsible for the odour quality of the product. Headspace analysis by SPME led to the traces shown in Figure 1, where visual inspection indicates a high degree of similarity between the two profiles. Forty-two peaks were identified using LRI and MS library spectra. When the peak areas of the 42 compounds were compared, only five showed significant differences in peak areas between the factory and laboratory samples. The SAFE extracts were analysed by GC-olfactometry by a single trained assessor and the same odour profile and similar odour intensities were reported for 68 peaks (see SI Figure SI-1 for details). Finally, a trained sensory panel assessed the odour of the factory product and the t_6 samples prepared using the laboratory-scale system. Using a robust sensory experimental design, no significant difference in the overall odour of the two samples was found at the 5% significance level (p = 0.518). From these data, it was

concluded that the laboratory and factory-generated products were similar to within the expected tolerances, and that the laboratory system was representative of the factory process.

3.2 FT-ICR-MS data acquisition

In a preliminary experiment, un-sterilised and fully-sterilised pet food extracts were infused into the FT-ICR-MS under positive and negative electrospray to assess which ionisation mode gave the best coverage of chemical compounds in the sample. Although positive ionisation produced more peaks than negative electrospray, the number of molecular formulae that could be calculated, and the number of identified compounds (using the KEGG database) were very similar for both positive and negative ionisation (See SI Table SI-1 for details). A similar effect was reported for cocoa bean analysis by FT-ICR-MS (Milev, Patras, Dittmar, Vrancken, & Kuhnert, 2014). Inspection of the data showed that many of the additional peaks in positive ionisation were due to the well-known phenomenon of adduct formation (e.g. addition of a sodium ion to a compound). For these reasons, negative electrospray ionisation was used for the next phase of the study.

A single sample extract was then analysed by FT-ICR-MS to check the mass resolution and coverage of the chemical classes in the sample. A region around *m/z* 271 was studied (See SI Figure SI-2 for details) and excellent mass resolution was achieved with the direct infusion method despite the chemical complexity of the sample. Elemental compositions were calculated and formulae with CHO, CHNO and CHNOS were clearly identified. Given existing knowledge about the chemical composition of pet food samples, the elements of importance were limited to CHNOPS and a colour code was adopted to allow easier identification of elemental compositions (see Figure 2).

3.2 Sample extraction

The sample extraction procedure was chosen to obtain wide coverage of the chemical classes present in pet food, as well as being relatively simple and quick, so that many samples (tens to hundreds) could be analysed. The coverage goal was achieved by simply defatting the pet food samples and using a methanol/water extract. Figure 2 shows that representatives of many chemical classes were present from CHO (e.g. sugars and fatty acids) through to CHNO (e.g. neutral and acidic amino acids/peptides) and CHNOS (e.g. peptides containing a sulfur amino acid) to CHNOP (e.g. nucleotides). Figure 2 shows the percentage distribution of the 1993 molecular formulae detected. What is not clear is where the cut-off point of this extraction system occurs in terms of compound hydrophilicity and hydrophobicity. Biological food systems generally contain hydrophilic small molecular weight compounds as well as much lower levels of hydrophobic volatile compounds. The current extraction protocol is well-aligned with the former compounds but, for the volatile hydrophobic compounds, it may be necessary to run a separate extraction using well-established methods like Solvent Assisted Flavour Evaporation (Engel, Bahr, & Schieberle, 1999).

3.3 Analytical variation

Seven samples were taken from the small-scale Parr system before (t_0), during (t_1 to t_5) and after (t_6) processing and the sterilisation process and sampling was repeated three times. After analysis by FT-ICR-MS and data cleaning, the data generated for each time point contained around 2000 molecular formulae with the corresponding ion intensities. Variation in the ion intensities for all molecular formulae was measured between replicates with over 90% of the masses having a percentage coefficient of variation (CV) less than 20%. In the small-scale Parr reactor system, the three

replicates were true biological replicates i.e. three different batches of meat chunks were selected, processed in three separate runs and 10-g samples taken at the different time points. Therefore, the heterogeneity of the raw materials, slight changes in processing conditions and variation in the timing of sampling, as well as the fact that the 10-g sample may contain different proportions of gravy and homogenised chunk, could combine to give the level of variation observed. The dilemma in this kind of experiment is that, although it is possible to decrease variation, in doing so, the experiment moves away from the reality of actual food products (which have some inherent variation) and does not represent what a pet will experience as it eats a pet food product chunk-by-chunk. This latter aspect was considered important from a commercial-relevance point of view. In addition, when comparing the differences in ion intensities for a specific molecular formula between time points (t_0 to t_6), the level of variation ranged from 90% CV to several orders of magnitude. Thus, the inherent analytical variation was relatively small compared to the changes generated by the sterilisation process over the time intervals. On this basis, the data were judged to be fit for purpose and were analysed without further changes, to establish whether they could follow chemical changes during processing in a reliable manner.

3.4 FT-ICR-MS data visualization and analysis

To view and interpret the data obtained, the molecular formulae (calculated from the accurate mass data) were plotted on van Krevelen diagrams (van Krevelen, 1950) on axes representing the oxygen to carbon (O:C) and hydrogen to carbon (H:C) ratios of each compound. The mean $\log_{10}$ ion intensity of each compound was represented by the size of the marker. Figure 3 shows a representation of all the data using H:C, O:C and time point as the x, y and z axes respectively. Some changes in ion intensities with processing time can already be observed from Figure 3 but, given the large number of molecular formulae present on the plots, visual analysis is very limited and it was necessary to develop a data analysis strategy and filter the data by various means.

3.5 Data mining to identify specific classes of chemicals

Software visualisation platforms like Spotfire® provide the ability to store (and carry out calculations) on large data sets and then visualise all or a subset of the data in a variety of 2D and 3D charts. Spotfire automatically sets up filters of all the data columns and these can be used to filter experimental data and search for specific classes of compounds. Filters were set up for H:C, O:C, N:C as well as the atom count for C, H, N, O, S and P. Some chemical classes have distinctive elemental signatures (see SI Table SI-3), which provide a means of isolating these classes of compounds from the mass of data shown in Figure 3. Filtering can use the ratios of H:C, O:C or N:C as well as using the number of atoms expected in a formula. As an initial example, the data were filtered to visualise the fatty acid profile of the data at one time point. Although the samples were defatted with hexane (which removes triglycerides) the fatty acids were expected to be present in the methanol-water extract analysed by FT-ICR-MS. By setting the oxygen count to O=2 and the carbon count to C>9 only the compounds meeting the filtering criteria were displayed, making the plots much easier to interpret (Figure 4). Inspection of the data in Figure 4 showed the compounds were arranged in what looked like homologous series of fatty acids of different chain lengths and degrees of unsaturation. The top row, with the generic formula $C_nH_{2n}O_2$ represents the saturated fatty acids and the subsequent lower rows represent mono-, di-, tri- *etc*. unsaturated fatty acids. By studying the molecular formulae, tentative annotation could be applied to the compounds and the pattern of the C18 fatty acids showing C18:0, C18:1, C18:2 and C18:3, as well as signals corresponding to C20:4 and

C22:6, were clear, and were very similar to fatty acid analyses from regular pet food. This initial example of filtering the data to isolate specific chemical classes (fatty acids in this case) from the thousands of compounds present at one time point, shows the power of filtering in analysing the FT-ICR-MS data. If filtering the data indicates there are interesting behaviours in the compounds during processing, then conventional, targeted analysis could be applied to provide unequivocal identification (and quantification) of the compounds of interest.

To further explore the range of chemical classes that could be identified by filtering, sulfur-containing pentapeptides were chosen for the next study. The pentapeptide backbone contains five nitrogen atoms, six oxygen atoms, while a sulfur amino acid will contribute one sulfur atom, so the signature of pentapeptides containing one S-amino acid and amino acids with aliphatic side chains (C, H only) will be N=5, O=6, S=1. Using this chemical signature as a filter, the data revealed the presence of several compounds with a carbon count between 22 and 26 (Figure 5).

Statistical analysis of the ion intensities between the time points using linear mixed models showed no significant differences, suggesting these particular masses originated from the raw materials and were not produced or hydrolysed during processing (data not shown). Closer examination of the N=5, O=6, S=1 and C=22 to 26 signature at one time point (t_6), revealed seven compounds with different molecular formulae (Figure 5). Taking the $C_{24}H_{45}N_5O_6S$ molecular formula, the amino acid composition could be Ala, Cys, $(Leu)_3$ (peptide A) or $(Val)_3$, Cys, Leu (peptide B) or Val, Met, $(Leu)_2$, Gly (peptide C). Obviously, ILeu could be substituted for Leu in these peptides as they have the same molecular mass. A tetrapeptide containing amino acids with hydroxyl, sulfur and amino groups could match the N_5O_6S signature (e.g. Lys, Thr, Met, Leu) but would not match the carbon count in the compounds shown in Figure 5. Therefore, a tetrapeptide structure is ruled out for these compounds.

Putative amino acid compositions for the other six molecular formulae in Figure 5 were assigned by calculating which amino acid substitutions to the three proposed amino acid compositions (Ala, Cys, $(Leu)_3$ (peptide A) or $(Val)_3$, Cys, Leu (peptide B) or Val, Met, $(Leu)_2$, Gly (peptide C)) would account for the mass differences observed. The mass differences between the molecular formulae in Figure 5 were equivalent to the loss of C_2H_4, the addition of CH_2 and the loss of 2H (Figure 5). Each mass change can be explained by single changes in the amino acid composition of the pentapeptide relative to $C_{24}H_{45}N_5O_6S$. Loss of C_2H_4 can be explained either by replacement of a Val residue by Ala in peptide B or C or the replacement of a Met residue in peptide C by a Cys residue. Addition of CH_2 to $C_{24}H_{45}N_5O_6S$ can be explained by replacing a Val residue with a Leu/ILeu residue in peptides A, B and C. Further addition of CH_2 can only be explained by replacement of another Val residue in peptide B by a Leu/ILeu residue. The difference of 2H can be explained by replacement of a Val residue by a Pro.

To determine what other compounds might share the six molecular formulae in Fig. 5, searches using PubChem were carried out to match the molecular formulae with chemical structures. The structures were related to a range of chemical classes e.g. non-proteinogenic pentapeptides (e.g. CID 20766220 & 59990493 with isovaline and ethyl side chains) or multi-heterocyclic ring compounds (CID 10029994 & 10839980) which bore little resemblance to the usual biological compounds found in food. A tetrapeptide (CID 118796813) with unusual substitutions at both ends of the peptide (acetyl and methylene thiol) was also not representative of a biological food source. In conclusion,

the PubChem database did not identify other classes of chemical compounds that might account for the related molecular formulae shown in Figure 5. Although these are theoretical explanations for the identity of the peptides filtered out of the data in this example, the fact that all the signatures can be related to feasible peptide compositions gives some credibility to their tentative identity as proteinogenic pentapeptides rather than the other structures found in PubChem for the molecular formula $C_{24}H_{45}N_5O_6S$. If these or other filtered compounds are of interest in the overall chemistry of a studied process, then they can be further investigated (qualified and quantified) using targeted analyses as proposed previously.

3.6 Filtering to identify chemical changes during processing

To explore whether FT-ICR-MS could measure the progress of the Maillard reaction during processing, the data were searched for molecular formulae and chemical changes that related to the first few steps of the Maillard reaction. From the published Maillard pathways (Belitz, Grosch, & Schieberle, 2009), it should be possible to see three initial molecular formulae that are distinct and amino-acid specific. These are the initial product when a reducing sugar and amino acid combine without the loss of mass (an addition reaction), then two dehydration steps that ultimately lead to the formation of the deoxyosones. The first dehydration produces a series of isomeric compounds, including the Schiff base, the N-substituted glycosylamine, the 1,2- and 2,3-enaminols and the Amadori compound. Further loss of water from the 1,2- and 2,3- enaminol compounds leads to two intermediate compounds, containing both amino acid and sugar residues. The next stage involves loss of the amino acid moiety to produce a range of sugar-derived, dicarbonyl compounds which can further react with amino acids in a second cycle of the reaction.

The formulae of the addition compounds as well as the single and double dehydration products for some common amino acids can be easily calculated (see SI Table SI-4 for details). For the twenty amino acids studied, molecular formulae corresponding to the addition compounds were found in the time-point data for all but four of the amino acids (Lys, Arg, Asn, Cys) as well as cystine. For the single dehydration product, Lys, Arg and Tyr were the amino acids with no corresponding molecular formulae. For the double dehydration product, corresponding molecular formulae were found for Thr, Arg, Ala, Asp, Cys, Glu, Gln, Gly, Ser, Tau, Asn and cystine but not for Tyr, Pro, His, Val, Try, Phe, Met, Lys or Leu/ILeu.

To illustrate the changes during processing, Figure 6 shows the change in the ion intensities for the molecular formula proposed as cystine (cysteine dimer) as well as its single and double dehydration products during sterilisation (no addition compound was present at the molecular formula of $C_{12}H_{24}N_2O_{10}S_2$). Since all the compounds have the same elemental compositions, arbitrary colour codes have been applied to differentiate the compounds. Different letters in each row indicate statistically significant changes in the ion intensity of the molecular formulae. As explained previously, although identification of the compounds is tentative, the data provide insights into potentially interesting areas of Maillard chemistry, which can be further investigated using targeted analyses like LC-MS^n.

4. Discussion and Conclusion

This study successfully developed a small-scale system to improve the speed and efficiency of monitoring chemical changes during sterilisation of food. The small-scale sterilisation process was

representative of the factory process and the ability to sample during processing allows investigations on the effect of different formulations, ingredients and processing conditions on the chemical profile of food at different stages of sterilisation. Previously, the use of pilot plant experiments combined with conventional chemical analyses were time-consuming and only delivered information on the chemical composition of targeted compounds before and after sterilisation. The new approach provides high-throughput processing and analysis of samples as well as untargeted chemical analyses of a wide range of chemical classes. This data-rich output was combined with data visualization, data mining and interrogation to tentatively identify some chemical pathways and the origins of some of the key chemical components of pet food.

The simple extraction protocol, followed by infusion into the FT-ICR-MS and negative electrospray ionisation, provided good coverage of the chemical classes present in pet food as well as good mass resolution despite the presence of many thousand compounds. The accurate mass data allowed more confidence in assigning molecular formulae with between 1600 and 2200 molecular formulae present in each processed sample. Assigning structures to the molecular formulae to identify the compounds present was enhanced by filtering the data for specific chemical signatures and then visualizing the data on 2D and 3D van Krevelen diagrams. The ability to assign chemical formulae that tentatively identify homologous fatty acid series, pentapeptides and the early Maillard reaction sequences indicates the value of the chemical formulae in annotating the data. For full identification and quantification of compounds of interest which change during thermal processing, selected samples could be reanalysed using conventional analyses.
Despite the qualitative nature of the technique, it was possible to monitor the increase and decrease of some inter-related compounds as shown by the reaction of cystine with a C6 sugar. Further data processing could use the network principles developed in metabolomics to show inter-relationships between compounds and increase the granularity of the data (Johnson, Ivanisevic, Benton, & Siuzdak, 2014).

The combination of FT-ICR-MS analysis and data visualisation software provides new opportunities to obtain and interrogate large, untargeted datasets. The ability to process datasets containing 10^5 to 10^6 variables (masses) across many samples and use chemical-signature filtering to isolate potential compounds of interest, then apply other tools like PCA or PLS to identify patterns in the data, opens up new areas for research.

REFERENCES:

Balagiannis, D. P., Howard, J., Parker, J. K., Desforges, N., & Mottram, D. S. (2010). Kinetic Modeling of the Formation of Volatile Compounds in Heated Beef Muscle Extracts Containing Added Ribose. In D. S. Mottram & A. J. Taylor (Eds.), *Controlling Maillard Pathways To Generate Flavors*, vol. 1042 (pp. 13-25). Washington DC: American Chemical Society.

Belitz, H.-D., Grosch, W., & Schieberle, P. (2009). *Food Chemistry* (4th ed.). Berlin: Springer Science & Business Media.

Chu, P. I., & Doyle, D. (1999). Development and evaluation of a laboratory-scale apparatus to simulate the scale-up of a sterile semisolid and effects of manufacturing parameters on product viscosity. *Pharmaceutical Development and Technology, 4*(4), 553-559.

Clark, K. D., Zhang, C., & Anderson, J. L. (2016). Sample Preparation for Bioanalytical and Pharmaceutical Analysis. *Anal Chem, 88*(23), 11262-11270.

Davidek, J., Velisek, J., & Pokorny, J. (1990). *Chemical changes during food processing*. Amsterdam: Elsevier Science Publishers.

Dunnett, C. W. (1955). A multiple comparison procedure for comparing several treatments with a control. *Journal of the American Statistical Association, 50*, 1096-1121.

Engel, W., Bahr, W., & Schieberle, P. (1999). Solvent assisted flavour evaporation - a new and versatile technique for the careful and direct isolation of aroma compounds from complex food matrices. *European Food Research and Technology, 209*(3-4), 237-241.

Garcia, J. S., Vaz, B. G., Corilo, Y. E., Ramires, C. F., Saraiva, S. A., Sanvido, G. B., Schmidt, E. M., Maia, D. R. J., Cosso, R. G., Zacca, J. J., & Eberlin, M. N. (2013). Whisky analysis by electrospray ionization-Fourier transform mass spectrometry. *Food Research International, 51*(1), 98-106.

Garrett, R., Vaz, B. G., Hovell, A. M. C., Eberlin, M. N., & Rezende, C. M. (2012). Arabica and Robusta Coffees: Identification of Major Polar Compounds and Quantification of Blends by Direct-Infusion Electrospray Ionization-Mass Spectrometry. *Journal of Agricultural and Food Chemistry, 60*(17), 4253-4258.

Golon, A., Kropf, C., Vockenroth, I., & Kuhnert, N. (2014). An Investigation of the Complexity of Maillard Reaction Product Profiles from the Thermal Reaction of Amino Acids with Sucrose Using High Resolution Mass Spectrometry. *Foods, 3*, 461-475.

Guan, Y. G., Wang, S. L., Yu, S. J., Yu, S. M., & Zhao, Z. G. (2012). Changes in the initial stages of a glucose-proline Maillard reaction model system influences dairy product quality during thermal processing. *Journal of Dairy Science, 95*(2), 590-601.

Hwang, C. F., Shahidi, F., Onodenalore, A. C., & Ho, C. T. (1997). Thermally generated flavors from seal protein hydrolysate. In F. Shahidi & K. R. Cadwallader (Eds.), *Flavor and Lipid Chemistry of Seafoods*, vol. 674 (pp. 76-84). Washington: Amer Chemical Soc.

Johnson, C. H., Ivanisevic, J., Benton, H. P., & Siuzdak, G. (2014). Bioinformatics: The Next Frontier of Metabolomics. *Analytical Chemistry*.

Kemp, S. E., Hollowood, T. A., & Hort, J. (2009). *Sensory Evaluation*: Wiley-VCH.

Kuhnert, N., Drynan, J. W., Obuchowicz, J., Clifford, M. N., & Witt, M. (2010). Mass spectrometric characterization of black tea thearubigins leading to an oxidative cascade hypothesis for thearubigin formation. *Rapid Communications in Mass Spectrometry, 24*(23), 3387-3404.

Lindinger, C., Labbe, D., Pollien, P., Rytz, A., Juillerat, M. A., Yeretzian, C., & Blank, I. (2008). When machine tastes coffee: instrumental approach to predict the sensory profile of espresso coffee. *Anal Chem, 80*(5), 1574-1581.

Milev, B. P., Patras, M. A., Dittmar, T., Vrancken, G., & Kuhnert, N. (2014). Fourier transform ion cyclotron resonance mass spectrometrical analysis of raw fermented cocoa beans of Cameroon and Ivory Coast origin. *Food Research International, 64*, 958-961.

Moskowitz, M. R., & Peterson, D. G. (2010). Hydroxycinnamic Acid - Maillard Reactions in Simple Aqueous Model Systems. In D. S. Mottram & A. J. Taylor (Eds.), *Controlling Maillard Pathways To Generate Flavors*, vol. 1042 (pp. 53-62). Washington DC: American Chemical Society.

Mottram, D. S. (1998). Flavour formation in meat and meat products: a review. *Food Chemistry, 62*(4), 415-424.

Porcari, A. M., Fernandes, G. D., Belaz, K. R. A., Schwab, N. V., Santos, V. G., Alberici, R. M., Gromova, V. A., Eberlin, M. N., Lebedev, A. T., & Tata, A. (2014). High throughput MS techniques for caviar lipidomics. *Analytical Methods, 6*(8), 2436-2443.

Roullier-Gall, C., Lucio, M., Noret, L., Schmitt-Kopplin, P., & Gougeon, R. D. (2014). How Subtle Is the "Terroir'' Effect? Chemistry-Related Signatures of Two "Climats de Bourgogne''. *Plos One, 9*(5), 11.

van Krevelen, D. W. (1950). Graphical-statistical method for the study of structure and reaction processes of coal. *Fuel, 29*, 269-284.

Wang, R., Yang, C., & Song, H. L. (2012). Key meat flavour compounds formation mechanism in a glutathione-xylose Maillard reaction. *Food Chemistry, 131*(1), 280-285.

Wu, Z. G., Rodgers, R. P., & Marshall, A. G. (2004). Characterization of vegetable oils: Detailed compositional fingerprints derived from electrospray ionization Fourier transform ion cyclotron resonance mass spectrometry. *Journal of Agricultural and Food Chemistry, 52*(17), 5322-5328.

Yeretzian, C., Jordan, A., Badoud, R., & Lindinger, W. (2002). From the green bean to the cup of coffee: investigating coffee roasting by on-line monitoring of volatiles. *European Food Research and Technology, 214*(2), 92-104.

Figure legends

Figure 1. Comparison of the TIC traces from GC-MS analysis of the headspace obtained from factory products (upper trace) and the laboratory scale product at t_6 (lower trace). Both products were manufactured using the same batches of ingredients.

Figure 2. The chemical classes detected in an extract of pet food sample (t_6) by FT-ICR-MS, expressed as the percentage of the total number (1993) of molecular formulae.

Figure 3. van Krevelen plot of all compounds before (t_0) during (t_1 to t_5) and after (t_6) sterilisation, expressed as their C:O and H:C ratios. The size of the marker is proportional to the mean ion intensity and the colours indicate molecular composition

Figure 4: van Krevelen plot showing data from the t_6 sample plotted on C:H and C:O axes and filtered in the software using C>9 and O=1 or 2. The spherical markers show homologous series of fatty acids which differ in chain length (horizontal direction) or by number of double bonds (vertical direction). Diameter of the spheres is proportional to the log ion intensity as measured by FT-ICR-MS. Numbers on the Figure represent the number of carbon atoms in each compound as calculated from the accurate mass values. The generalised formulae (e.g. $C_nH_{2n}O_2$) denote the different fatty acid series with zero to six double bonds, each series is connected by a straight line to aid visualization of the homologous series. The size of the marker is proportional to the mean ion intensity of the three replicates.

Figure 5. Expanded van Krevelen plot of compounds with chemical signature C = 24 to 26, N = 5, O= 6, S= 1 at t_6 to show the chemical inter-relationships between the compounds. The potential fit with different amino acid compositions in the seven proposed pentapeptides is given in the text. The size of the marker is proportional to the mean $\log_{10}$ ion intensity (n=3).

Figure 6. van Krevelen diagram monitoring the molecular masses that correspond to the early stages of the Maillard reaction between cystine (cysteine dimer) and C6 sugar during processing. The top line shows the change in ion intensity of the amino acid cystine; the middle line shows the changes in the products of the condensation of cystine-C6 sugar and the bottom line shows the changes in the dehydration product of the cystine-C6 sugar product. The size of the marker is proportional to the ion intensity and the markers in the same row with different letters are statistically significantly different with respect to ion intensity. As all compounds are composed of CHNOS, colour codes have been changed to differentiate the different masses. Values are the means of three replicates, statistical analysis is described in Materials and Methods.

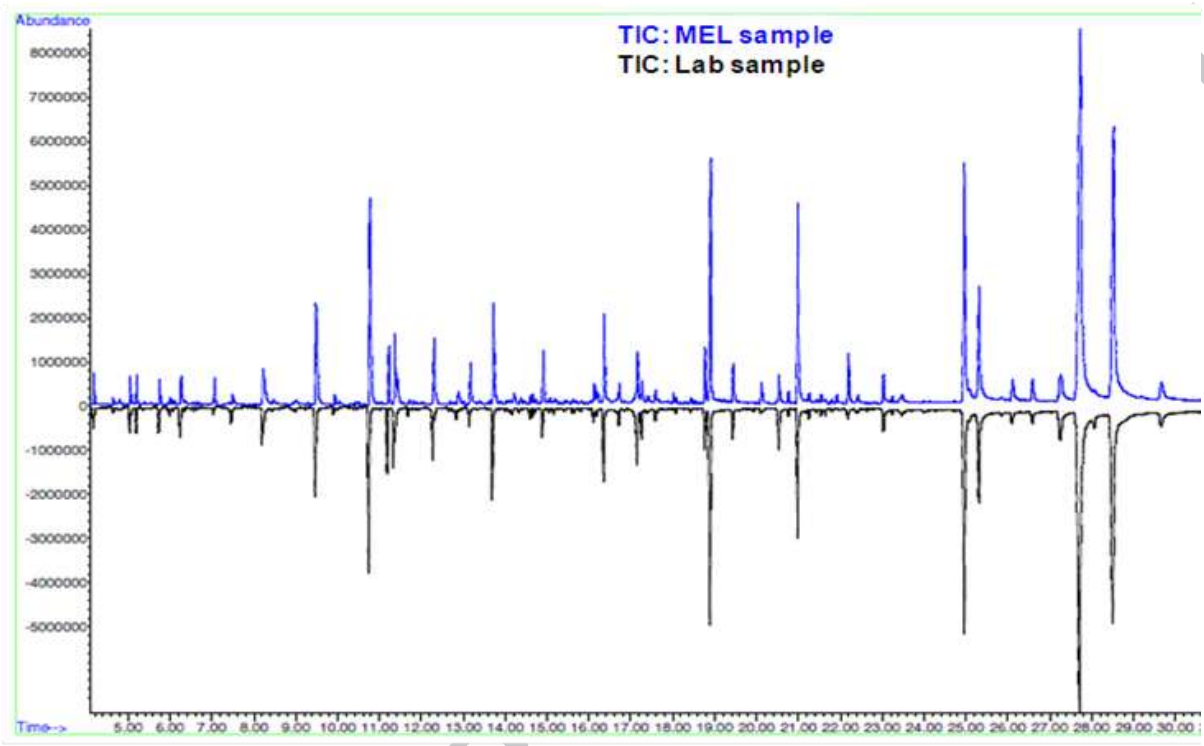

Figure 1. Comparison of the TIC traces from GC-MS analysis of the headspace obtained from factory products (upper trace) and the laboratory scale product at t_6 (lower trace). Both products were manufactured using the same batches of ingredients.

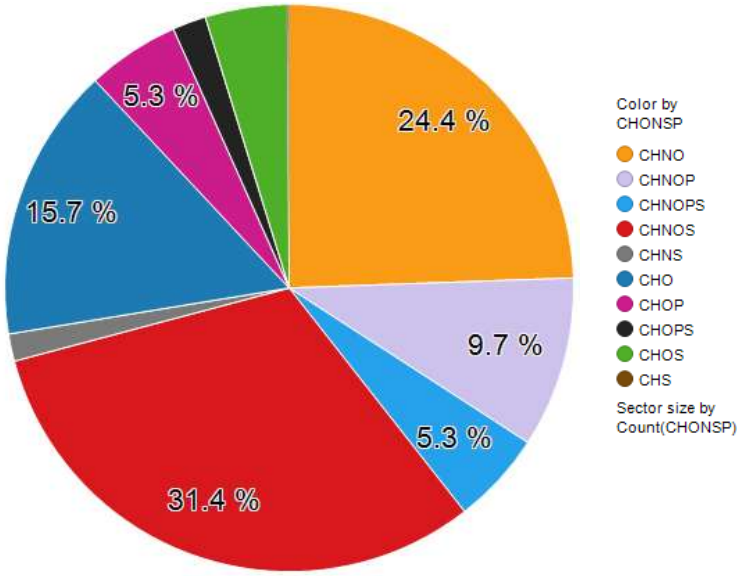

Figure 2. The chemical classes detected in an extract of pet food sample (t_6) by FT-ICR-MS, expressed as the percentage of the total number (1993) of molecular formulae.

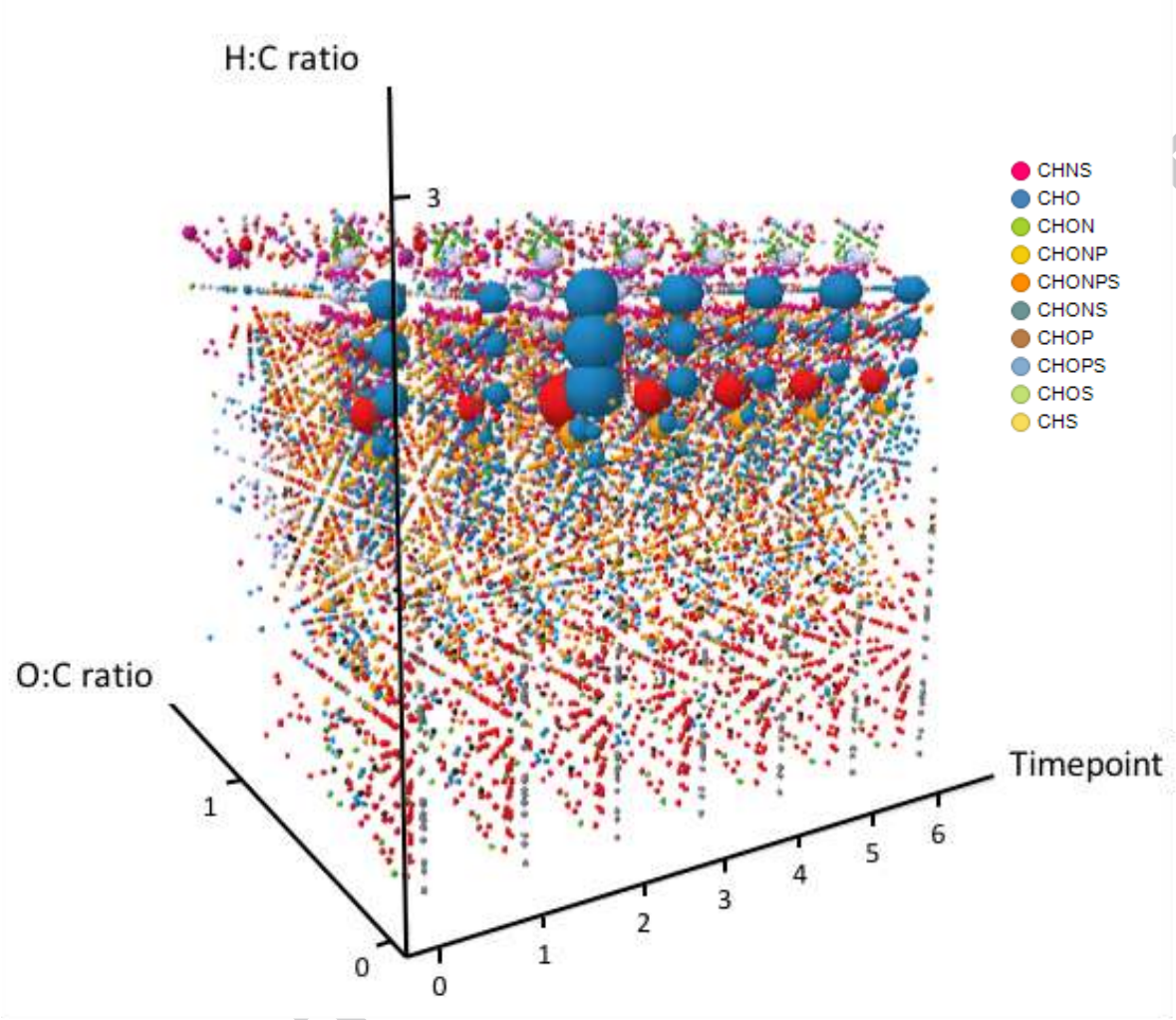

Figure 3. van Krevelen plot of all compounds before (t_0) during (t_1 to t_5) and after (t_6) sterilisation, expressed as their C:O and H:C ratios. The size of the marker is proportional to the mean ion intensity and the colours indicate molecular composition

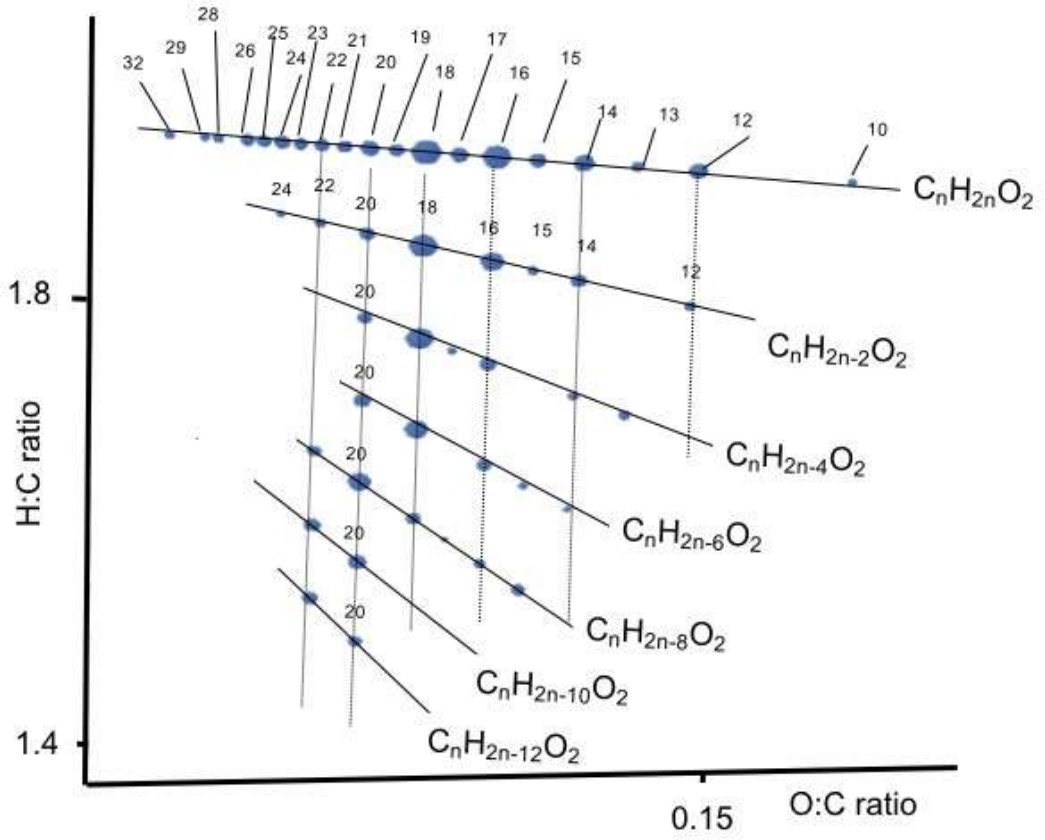

Figure 4: van Krevelen plot showing data from the t_6 sample plotted on C:H and C:O axes and filtered in the software using C>9 and O=1 or 2. The spherical markers show homologous series of fatty acids which differ in chain length (horizontal direction) or by number of double bonds (vertical direction). Diameter of the spheres is proportional to the log ion intensity as measured by FT-ICR-MS. Numbers on the Figure represent the number of carbon atoms in each compound as calculated from the accurate mass values. The generalised formulae (e.g. $C_nH_{2n}O_2$) denote the different fatty acid series with zero to six double bonds, each series is connected by a straight line to aid visualization of the homologous series. The size of the marker is proportional to the mean ion intensity of the three replicates.

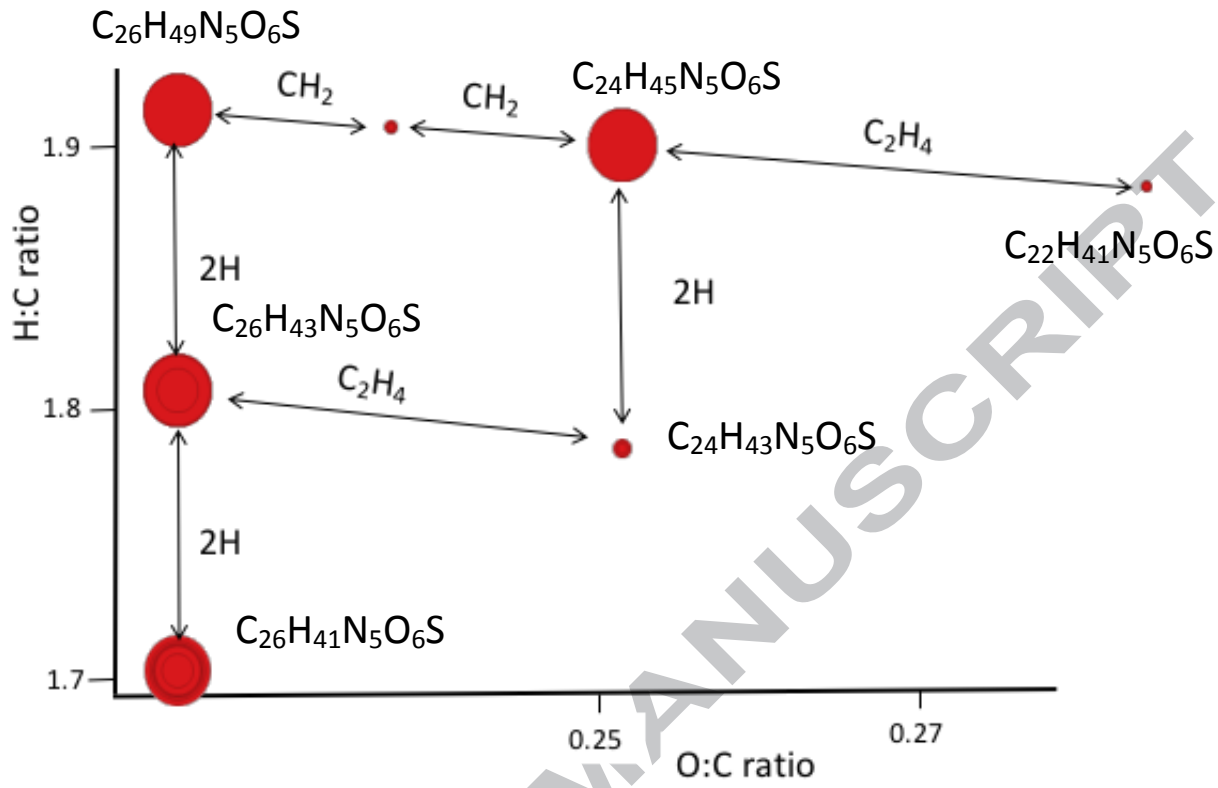

Figure 5. Expanded van Krevelen plot of compounds with chemical signature C = 24 to 26, N = 5, O= 6, S= 1 at t_6 to show the chemical inter-relationships between the compounds. The potential fit with different amino acid compositions in the seven proposed pentapeptides is given in the text. The size of the marker is proportional to the mean $\log_{10}$ ion intensity (n=3).

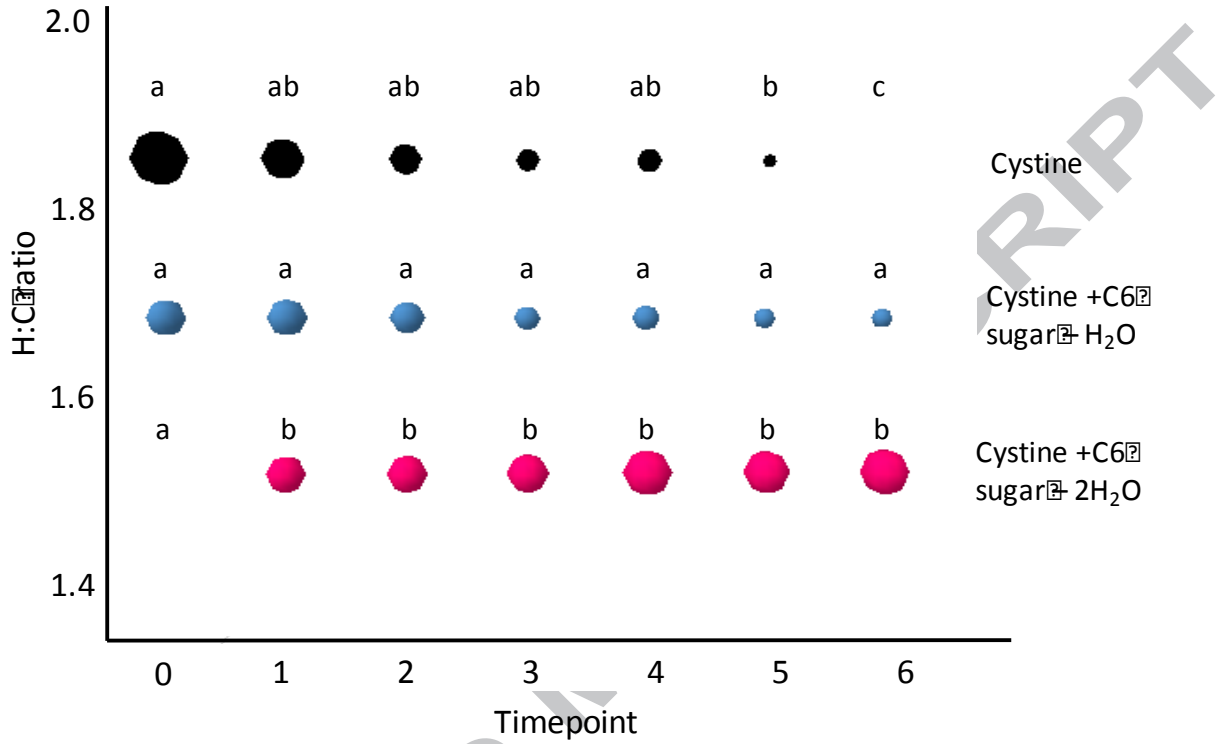

Figure 6. van Krevelen diagram monitoring the molecular masses that correspond to the early stages of the Maillard reaction between cystine (cysteine dimer) and C6 sugar during processing. The top line shows the change in ion intensity of the amino acid cystine; the middle line shows the changes in the products of the condensation of cystine-C6 sugar and the bottom line shows the changes in the dehydration product of the cystine-C6 sugar product. The size of the marker is proportional to the ion intensity and the markers in the same row with different letters are statistically significantly different with respect to ion intensity. As all compounds are composed of CHNOS, colour codes have been changed to differentiate the different masses. Values are the means of three replicates, statistical analysis is described in Materials and Methods.

Highlights

- Laboratory-scale system allowed monitoring of chemical changes during sterilisation
- The lab-scale process was representative of the factory pet food process
- FT-ICR-MS indicated around 2000 molecular formulae were present in each sample
- Data visualisation allowed tentative identification of some compounds
- The first stages of reaction between amino acids and sugars were monitored